ORIGINAL ARTICLE

Particulate Matter Induces NLRP3 Inflammasome-Mediated Pyroptosis in Human Nasal Epithelial Cells

Hosung Choi, MD[1], Hyunsu Choi, MS[2], Jeong-Min Oh, MS[2], and Dong Chang Lee, MD, PhD[1]

[1]Department of Otorhinolaryngology-Head and Neck Surgery, College of Medicine, The Catholic University of Korea, Seoul, Republic of Korea
[2]Clinical Research Institute, Daejeon St. Mary's Hospital, Daejeon, Republic of Korea

Background and Objectives: Air pollution, particularly particulate matter (PM), has a variety of adverse effects on human health. PM is known to induce cell death through various pathways, including pyroptosis. Despite its significance, research on PM-induced pyroptosis in nasal epithelial cells remains limited. This study aimed to explore PM-induced pyroptosis in cultured human nasal epithelial cells.

Methods: For the in vitro experiments, human nasal epithelial cells were cultured. Cell viability was assessed using a 3-(4,5-dimethyl-thiazol-2-yl)-2,5-diphenyltetrazolium bromide (MTT) assay, while cell death was evaluated through propidium iodide (PI) staining and lactate dehydrogenase (LDH) release measurement. Protein expression levels related to pyroptosis were examined via western blot using antibodies against NOD-like receptor family, pyrin domain containing 3 (NLRP3), cleaved caspase-1 (CASP1 P20), gasdermin D (GSDMD)-N, and glyceraldehyde phosphate dehydrogenase. Immunofluorescent staining with a CASP1 P20 antibody was conducted to visualize cellular localization. Enzyme-linked immunosorbent assay was utilized to quantify interleukin (IL)-1β and IL-18 protein levels.

Results: Treatment with PM resulted in decreased cell viability, elevated LDH release, and intensified PI staining, indicating cell death. Pyroptosis was confirmed by the elevated expression of NLRP3, CASP1 P20, and GSDMD-N, along with increased levels of IL-1β and IL-18. Inhibiting the NLRP3 inflammasome with MCC950 reduced the PM-induced effects on protein expression and cytokine release, highlighting the role of the NLRP3 inflammasome in PM-triggered pyroptosis in human nasal epithelial cells.

Conclusion: We showed that PM triggers pyroptosis in human nasal epithelial cells, driven by NLRP3 inflammasome-dependent signaling pathways.

Keywords: Particulate matter; Pyroptosis; Inflammasomes; Nasal mucosa.

INTRODUCTION

There has recently been growing interest in the adverse impacts of air pollution on human health. Particulate matter (PM), one of key components of air pollution, is categorized into PM_{10} (diameter smaller than 10 μm), $PM_{2.5}$ (diameter smaller than 2.5 μm), and $PM_{0.1}$ (diameter smaller than 0.1 μm) according to its aerodynamic diameter [1,2]. The health effects of PM vary depending on its size; smaller particles can penetrate and accumulate in the lower respiratory tract, and

particles smaller than 1 μm can even diffuse into the circulation through the alveoli and deposit in cell tissue [3-5]. Numerous studies have explored the detrimental health impacts of PM, which include cardiovascular, respiratory, neurological, and reproductive system diseases [6-11]. PM generates oxidative stress through the production of reactive oxygen species (ROS), leading to inflammatory responses and cell death [12-15]. It can trigger cell death in various organs via multiple pathways, including necrosis, apoptosis, autophagy, pyroptosis, and ferroptosis [16]. Among the various patterns of cell death, pyroptosis is a relatively recently discovered inflammatory cell death process characterized by nuclear condensation, cell swelling, and plasma membrane rupture without DNA fragmentation [17]. Various stimuli, including pathogen-associated molecular patterns and damage-associated molecular patterns, induce the formation of the NOD-like receptor family, pyrin domain containing 3 (NLRP3) inflammasome complex. This complex generates mature caspase-1, which pro-

duces the pro-inflammatory cytokines interleukin (IL)-1β and IL-18 by cleaving pro-IL-1β and pro-IL-18, respectively. Additionally, it triggers the cleavage of gasdermin D (GSD-MD), leading to the formation of GSDMD-N. GSDMD-N binds to phospholipids on the plasma membrane, forming pores that induce pyroptosis [17,18]. Some studies have suggested that PM induces tissue injury through pyroptosis, demonstrating its role in conditions such as neuronal injury, myocardial injury, renal tubular injury, lung injury, and corneal injury [9,19-22]. However, few attempts have been made to investigate pyroptosis induced by PM in nasal epithelial cells. This study investigated PM-induced pyroptosis and the underlying signaling mechanisms in human nasal epithelial cells.

METHODS

Ethics
The study protocol was approved by the Institutional Review Board of Daejeon St. Mary's Hospital (IRB policy No. DC15TISI0022, 22 May 2020).

Reagents
Antibiotic-antimycotic solution, fetal bovine serum (FBS) solution, and Eagle's Minimum Essential Medium (EMEM) were sourced from Gibco, a brand of Thermo Fisher Scientific (Waltham, MA, USA). The lactate dehydrogenase (LDH) assay, IL-1β and IL-18 enzyme-linked immunosorbent assay (ELISA) kits, and 4',6-diamidino-2-phenylindole (DAPI) were purchased from Abcam (Cambridge, UK). The PM standard reference material SRM 2786, MCC950, and propidium iodide (PI) were obtained from Millipore Sigma-Aldrich (Saint Louis, MO, USA). Antibodies specific for NLRP3, glyceraldehyde phosphate dehydrogenase (GAPDH), and cleaved caspase-1 were procured from Cell Signaling Technology (Danvers, MA, USA). Additionally, the antibody targeting GSDMD-N was acquired from Abcam.

Preparation of the PM solutions
The PM standard reference material SRM 2786 (Millipore Sigma-Aldrich, St. Louis, MO, USA) was dispersed in phosphate-buffered saline (PBS) to achieve a final concentration of 100 μg/mL. It was then further diluted to 50 μg/mL and 25 μg/mL and subjected to 30 minutes of ultrasonication prior to treatment. These concentrations were selected based on the study conducted by Wang et al. [23].

Cell culture
Human nasal epithelial RPMI-2650 cells (ATCC#CCL-30, ATCC, Manassas, VA, USA) were cultured in EMEM (ATCC# 30-2003) supplemented with 1% antibiotic-antimycotic solution and 10% FBS. The culture medium was refreshed every 2–3 days to maintain cell integrity and provide essential nutrients. The cells were incubated in a humidified environment to ensure optimal conditions for growth.

Detection of cell viability
To assess cell viability and cytotoxicity, we performed a 3-(4,5-dimethylthiazol-2-yl)-2,5-diphenyltetrazolium bromide (MTT) assay using an EZ-Cytox Cell Viability Assay Kit (DoGen, Seoul, Republic of Korea). We applied 10 μL of the MTT assay kit reagent to each well containing the cells after the designated treatment. The plate was then incubated for an additional 2 hours to allow the conversion of MTT into formazan crystals by viable cells. Subsequently, the absorbance of the formazan product was measured at a wavelength of 450 nm using a microplate reader (Bio-Rad, Hercules, CA, USA).

Cell death analysis (PI and LDH release)
To evaluate pore formation in cell membranes, PI staining was conducted. Following the treatment, the cells were stained with a PI mixture and incubated for 25 minutes at 37°C. The stained cells were subsequently observed and imaged using a fluorescence microscope. To assess cell membrane damage, LDH release was measured. Cell culture supernatants were collected after the specified treatment, and LDH release was quantified using an LDH Kit according to the manufacturer's guidelines.

Western blot
To extract proteins, cells were rinsed with PBS and lysed using radioimmunoprecipitation assay buffer (Elpis Biotech, Daejeon, Korea) supplemented with protease inhibitors (Roche Diagnostics, Mannheim, Germany). The lysates were then centrifuged for 15 minutes at 13,000 rpm to isolate the protein fraction. Protein concentration was determined using a bicinchoninic acid protein assay kit from Pierce (Rockford, IL, USA). Equal amounts of proteins were separated by sodium dodecyl sulfate-polyacrylamide gel electrophoresis and transferred onto nitrocellulose membranes (Bio-Rad). The membranes were incubated overnight at 4°C with primary antibodies against NLRP3 (1:500), GSDMD-N (1:500), caspase-1 (P20, 1:500), and GAPDH (1:1,000). Subsequently, the membranes were treated with horseradish peroxidase-conjugated secondary antibody and the signals were developed using an enhanced chemiluminescence reaction. Positive bands were detected using a ChemiDoc XRS+ system (Bio-Rad).

Immunofluorescence staining
After rinsing the cells with PBS, they were fixed with a 4%

paraformaldehyde solution for 15 minutes. The cells were then permeabilized with a 0.2% Triton-X-100 solution at room temperature for 15 minutes. Subsequently, the cells were blocked with 5% bovine serum albumin for 1 hour to prevent nonspecific antibody binding and reduce background signal. The primary antibody against caspase-1 (P20) was added at a 1:200 dilution, and the cells were incubated overnight at 4°C. Following another wash, the cells were treated with an anti-rabbit Alexa Fluor 488 secondary antibody at a 1:1,000 dilution and incubated in the dark for 1 hour at room temperature. To visualize the nuclei, the cells were stained with DAPI for 10 minutes. The stained cells were examined using an Olympus IX73 fluorescence microscope (Olympus Corp., Tokyo, Japan). For quantitative analysis of immunofluorescence intensity, the images were processed using ImageJ software (version 1.54g; National Institutes of Health, Bethesda, MD, USA).

Enzyme-linked immunosorbent assay

IL-1β and IL-18 protein levels in the culture supernatant were measured using ELISA kits, following the manufacturer's instructions. The concentrations of IL-1β and IL-18 were determined by correlating the absorbance values with a standard curve, which was created using known concentrations of recombinant cytokines.

Pretreatment with MCC950

To demonstrate that PM-induced pyroptosis occurs via the NLRP3 inflammasome-dependent pathway, cells were first pretreated with 1 μM MCC950, an inhibitor of the NLRP3 inflammasome, for 2 hours. Subsequently, they were exposed to the lowest concentration of PM that demonstrated a significant difference from the control group in a western blot analysis. This was followed by an additional 24-hour incubation period. The 1 μM concentration of MCC950 used in this study was based on the dosage reported in the paper by Roseborough et al. [24].

Statistical analysis

All experiments were conducted independently three times, with one representative experiment displayed. Data analysis was carried out using GraphPad Prism 5 software (GraphPad, Inc., La Jolla, CA, USA). Depending on the experimental design, the statistical significance of differences between control and experimental values was assessed using either the unpaired t-test or one-way analysis of variance (ANOVA). All data were presented as mean±standard error of the mean (SEM).

RESULTS

Effect of PM on the viability of human nasal epithelial cells

Cell viability was assessed using the MTT assay after a 24-hour exposure to various PM concentrations (0, 25, 50, or 100 μg/mL). We observed significant reductions in cell viability at PM concentrations of 50 μg/mL or higher, compared to the control group (p<0.05) (Fig. 1A). Similarly, LDH release, which indicates cell death, increased significantly at PM concentrations of 50 μg/mL or higher. This increase in LDH release was more pronounced at higher PM concentrations (p<0.05) (Fig. 1B), suggesting a dose-dependent increase in cell death. Additionally, PI staining, used to confirm cell death, showed higher staining intensity at higher PM concentrations, as observed through fluorescence microscopy (Fig. 1C).

Pyroptosis in human nasal epithelial cells induced by PM

After exposing the cells to various PM concentrations (0, 25, 50, or 100 μg/mL) for 24 hours, we conducted western blot analysis to evaluate the expression levels of key proteins involved in NLRP3 inflammasome activation: cleaved caspase-1 (CASP1 P20), NLRP3, and GSDMD-N (Fig. 2A). The protein levels of NLRP3, CASP1 P20, and GSDMD-N, relative to the GAPDH control, were significantly elevated at PM concentrations of 50 μg/mL or higher compared to the control (p<0.05) (Fig. 2B-D). Additionally, immunofluorescence staining showed increased expression levels of CASP1 P20 with rising PM concentrations (Fig. 2E). ELISA analysis of the cell culture supernatants indicated a significant increase in IL-1β and IL-18 protein levels at PM concentrations of 25 μg/mL or higher compared to the control, with the intensity of release increasing as PM concentration rose (p<0.05) (Fig. 2F and G). In summary, these findings suggest that PM induces pyroptosis in human nasal epithelial cells.

PM provoked pyroptosis of human nasal epithelial cells in an NLRP3 inflammasome-dependent manner

Cells were pretreated with 1 μM MCC950, an NLRP3 inflammasome inhibitor, for 2 hours before being exposed to 50 μg/mL of PM, followed by an additional 24-hour incubation. The increased western blot signals of CASP1 P20, NLRP3, and GSDMD-N observed in cells exposed to 50 μg/mL of PM, compared to the control, were reversed following the addition of MCC950 (Fig. 3A). Pretreatment with MCC950 led to a significant reduction in the expression levels of NLRP3, CASP1 P20, and GSDMD-N compared to treatment with PM alone (p<0.05) (Fig. 3B-D). Immunofluorescence staining further
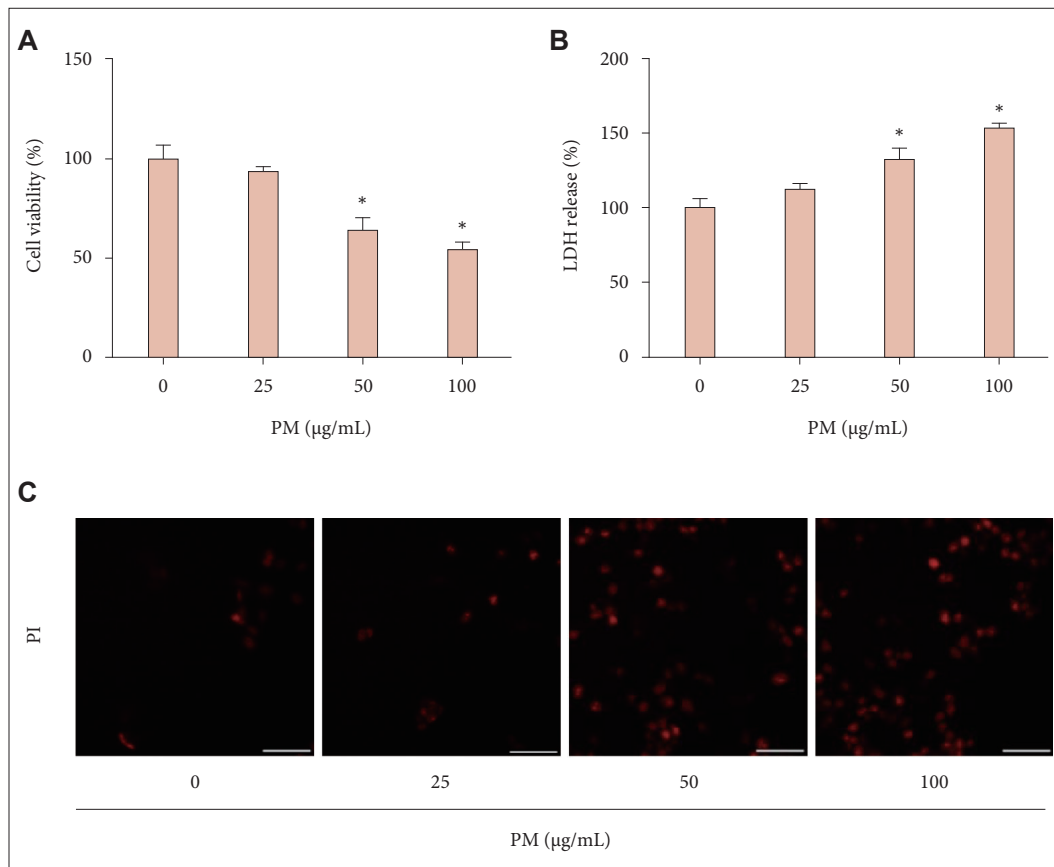
Fig. 1. PM induced cell death. A: Cell viability was assessed using the MTT assay after treating the cells with different concentrations of PM (0, 25, 50, or 100 µg/mL) for 24 hours. The MTT assay showed a significant decrease in cell viability with increasing concentrations of PM exposure. B: Cell death was evaluated using the LDH assay after exposing the cells to PM at varying concentrations for 24 hours. The LDH assay indicated a notable induction of cell death in response to PM exposure. C: Cell death was further confirmed using PI staining. After 24 hours of exposure to PM, the cells were stained with PI to visualize dead cells. The PI staining results confirmed that PM exposure induced cell death in human nasal epithelial cells. The experiment was performed three times. For all experiments, data are presented as mean±SEM of the results from three individual experiments. *$p<0.05$ compared to the untreated control; Scale bar= 50 µm. PM, particulate matter; MTT, 3-(4,5-dimethylthiazol-2-yl)-2,5-diphenyltetrazolium bromide; LDH, lactate dehydrogenase; PI, propidium iodide.

demonstrated decreased expression levels of CASP1 P20 in samples treated with both MCC950 and PM compared to those treated with PM alone (Fig. 3E). ELISA analysis indicated that the elevated release of IL-1β and IL-18 observed in samples treated with 50 µg/mL of PM was significantly reduced following the addition of MCC950 ($p<0.05$) (Fig. 3F and G).

DISCUSSION

In this study, we found that PM induces cell death in cultured human nasal epithelial cells through the process of pyroptosis, characterized by a significant increase in the protein levels of NLRP3, CASP1 P20, GSDMD-N, IL-1β, and IL-18. Pretreatment with MCC950, an inhibitor of the NLRP3 inflammasome, resulted in decreased levels of these proteins, suggesting that PM-triggered pyroptosis is mediated by the NLRP3 inflammasome-dependent pathway.

Ren et al. [25] found that $PM_{2.5}$ initiated NLRP3 inflammasome-mediated pyroptosis by generating ROS in both murine macrophage cells in vitro and mouse lung tissue in vivo. They demonstrated that the addition of the ROS scavenger N-acetyl cysteine led to a reduction in proteins associated with pyroptosis, indicating that ROS generation triggers pyroptosis induced by $PM_{2.5}$. Similarly, Li et al. [22] reported that exposure to $PM_{2.5}$ activated the NLRP3/caspase-1 signaling pathway, causing macrophage pyroptosis and subsequent inflammation and injury in the lung tissue of a mouse model. Zheng et al. [26] also confirmed the activation of the NLRP3 inflammasome pathway by $PM_{2.5}$ through mechanisms such as ROS production, K^+ efflux from plasma membrane perturbation, and cathepsin B release due to lysosomal damage, using human monomyelocytic leukemia cell lines. Additionally, they showed that $PM_{2.5}$ induces pulmonary fibrosis in mice. In re-
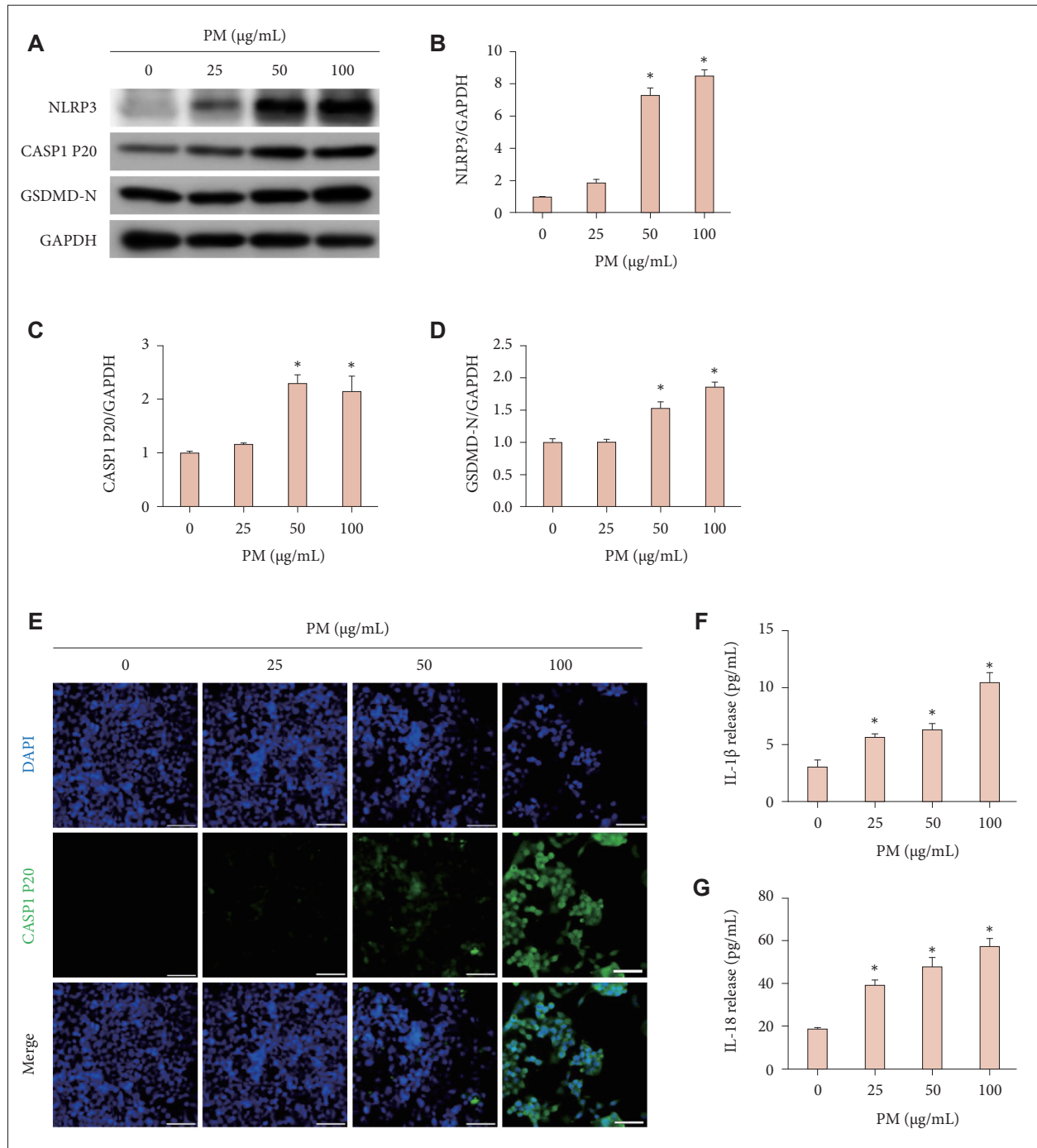
Fig. 2. PM exposure induced pyroptosis in human nasal epithelial cells. The cells were treated with varying concentrations of PM (0, 25, 50, or 100 μg/mL) for 24 hours. A: Western blot analysis assessed the expression levels of key proteins involved in NLRP3 inflammasome activation, including NLRP3, cleaved caspase-1, and GSDMD-N. B-D: The western blot signals were quantified, and the relative intensity of protein levels compared to the GAPDH control was determined. At PM concentrations of 50 μg/mL or higher, the levels of NLRP3, cleaved caspase-1, and GSDMD-N significantly increased compared to the control. E: Immunofluorescence staining was used to assess the expression levels of cleaved caspase-1, a key protein in NLRP3 inflammasome activation. Nuclei were counterstained with DAPI. The expression levels of cleaved caspase-1 increased proportionally with the PM concentration. F and G: ELISA was conducted to measure the release of IL-1β and IL-18, two pro-inflammatory cytokines, in the cell culture supernatant. The release of IL-1β and IL-18 increased compared to the control following PM application. For all experiments, data are presented as mean±SEM from three individual experiments. *p<0.05 compared to the untreated control; Scale bar=50 μm. PM, particulate matter; NLRP3, NOD-like receptor family, pyrin domain containing 3; CASP1 P20, cleaved caspase-1; GSDMD, gasdermin D; GAPDH, glyceraldehyde phosphate dehydrogenase; DAPI, 4',6-diamidino-2-phenylindole; ELISA, enzyme-linked immunosorbent assay; IL, interleukin.
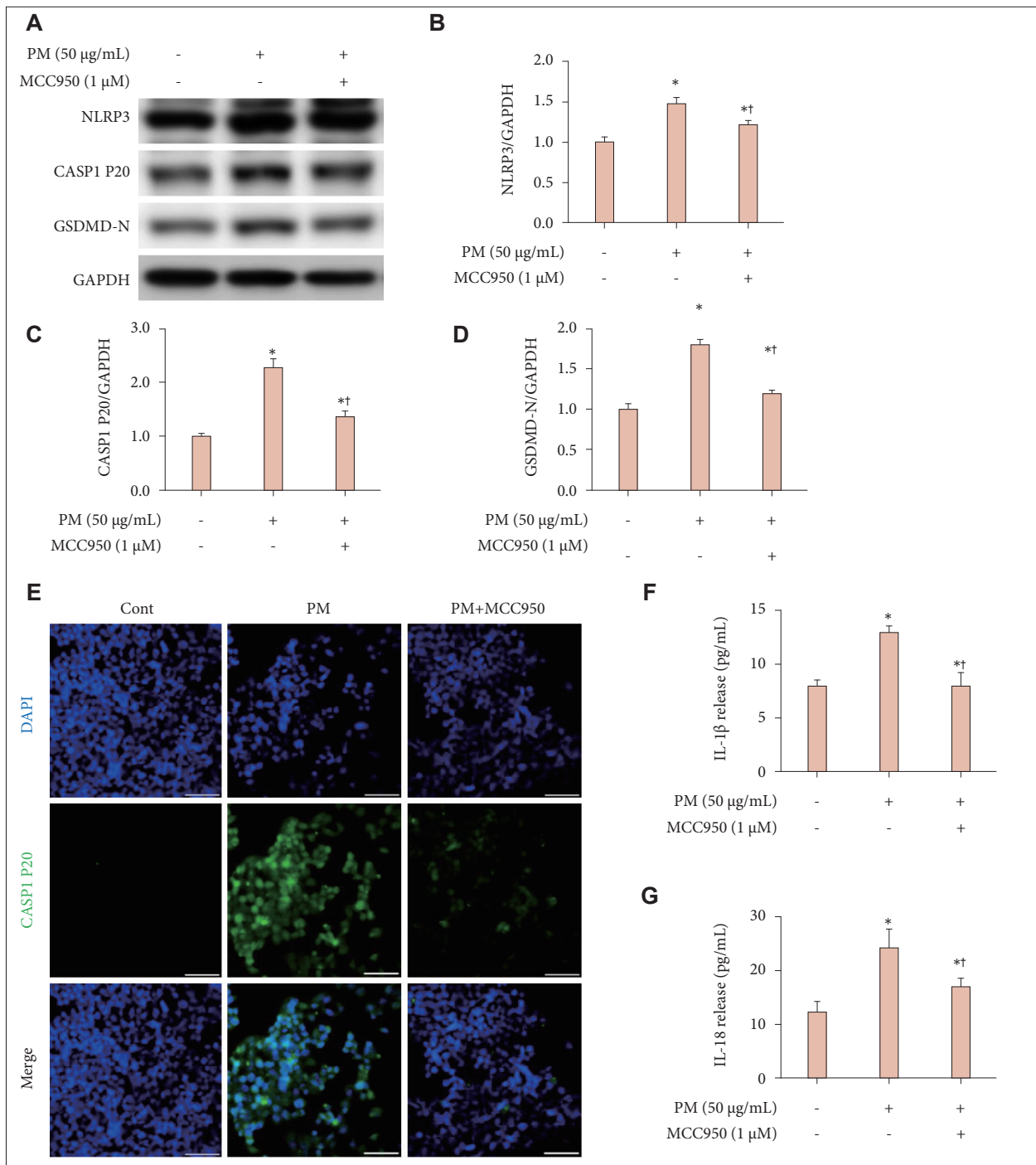
Fig. 3. PM induced pyroptosis in human nasal epithelial cells in an NLRP3 inflammasome-dependent manner. Cells were pretreated with MCC950 at a concentration of 1 µM for 2 hours before the addition of PM at a concentration of 50 µg/mL. Following PM exposure, the cells were incubated for an additional 24 hours. A: Western blot analysis was conducted to assess the expression levels of NLRP3, cleaved caspase-1, and GSDMD-N. B-D: The western blot signals were quantified, showing that MCC950 pretreatment resulted in reduced expression levels of NLRP3, cleaved caspase-1, and GSDMD-N compared to treatment with PM alone. E: Immunofluorescence staining was used to evaluate the expression levels of cleaved caspase-1, with nuclei counterstained using DAPI. The expression levels of cleaved caspase-1 were lower following MCC950 pretreatment than with PM treatment alone. F and G: ELISA was utilized to measure the release of IL-1β and IL-18. MCC950 pretreatment also led to a reduction in the release of IL-1β and IL-18 compared to PM treatment alone. For all experiments, data are presented as mean ± SEM from three individual experiments. *p<0.05 compared to the untreated control and †p<0.05 compared to the PM alone-treated group; scale bar=50 µm. PM, particulate matter; NLRP3, NOD-like receptor family, pyrin domain containing 3; CASP1 P20, cleaved caspase-1; GSDMD, gasdermin D; GAPDH, glyceraldehyde phosphate dehydrogenase; DAPI, 4',6-diamidino-2-phenylindole; ELISA, enzyme-linked immunosorbent assay; IL, interleukin.

search focusing on the upper respiratory tract, Li et al. [27] demonstrated that $PM_{2.5}$ exacerbated allergic rhinitis symptoms and triggered pyroptosis through NLRP3, caspase-1, and GSDMD-dependent pathways, using an allergic rhinitis mouse model. Another study by Li et al. [28] showed that IL-17A mediated pyroptosis in human nasal epithelial cells via the extracellular signal-regulated kinase (ERK)-NLRP3/caspase-1 pathway, although it did not explore the effects of PM.

Our study, in line with the above findings, appears to be the first to specifically demonstrate that PM induces NLRP3 inflammasome-driven pyroptosis in cultured human nasal epithelial cells. To our knowledge, this has not been previously reported in the literature, marking our research as a novel contribution to understanding the effects of PM on this particular cell type. The use of MCC950, a specific NLRP3 inflammasome inhibitor, provides further insight into our findings. MCC950's ability to attenuate PM-induced pyroptosis underscores the critical role of the NLRP3 inflammasome pathway in this process. This finding not only supports existing studies on the role of the NLRP3 inflammasome in PM-triggered pyroptosis, but also suggests potential therapeutic interventions targeting this pathway to mitigate the detrimental health effects of PM exposure.

However, there are some limitations to our study. SRM 2786, the PM standard reference material used, contains a variety of organic and inorganic components of different sizes, including $PM_{2.5}$ and PM_{10} [29]. Therefore, it is unclear which specific component is the causative agent of NLRP3 inflammasome-mediated pyroptosis. Additionally, since cell death induced by PM can occur through various pathways such as necrosis, apoptosis, autophagy, pyroptosis, and ferroptosis, the observed decrease in cell viability may not be solely attributable to pyroptosis, as other pathways may also contribute. Consequently, it was impossible to quantify the specific contribution of pyroptosis to cell death [16]. Lastly, due to the in vitro nature of this study, we were unable to determine how PM-triggered pyroptosis would occur in human nasal epithelial cells under actual in vivo conditions. Future studies are therefore warranted to investigate whether PM causes pyroptosis in human nasal epithelial cells in vivo and to determine which particle composition and size are responsible for pyroptosis. Based on these findings, we anticipate that future research will explore the therapeutic potential of compounds targeting pyroptosis signaling pathways to alleviate the adverse effects of PM exposure on human health.

Availability of Data and Material

The datasets generated or analyzed during the study are available from the corresponding author on reasonable request.

ORCID iDs

Hosung Choi	https://orcid.org/0009-0000-9871-3495
Hyunsu Choi	https://orcid.org/0000-0002-9502-494X
Jeong-Min Oh	https://orcid.org/0009-0003-5553-2549
Dong Chang Lee	https://orcid.org/0000-0002-7917-4390

REFERENCES

1) Atkinson RW, Fuller GW, Anderson HR, Harrison RM, Armstrong B. Urban ambient particle metrics and health: a time-series analysis. Epidemiology 2010;21(4):501-11.
2) Hasheminassab S, Daher N, Schauer JJ, Sioutas C. Source apportionment and organic compound characterization of ambient ultrafine particulate matter (PM) in the Los Angeles Basin. Atmos Environ 2013; 79:529-39.
3) Kim KH, Kabir E, Kabir S. A review on the human health impact of airborne particulate matter. Environ Int 2015;74:136-43.
4) Löndahl J, Pagels J, Swietlicki E, Zhou J, Ketzel M, Massling A, et al. A set-up for field studies of respiratory tract deposition of fine and ultrafine particles in humans. J Aerosol Sci 2006;37(9):1152-63.
5) Valavanidis A, Fiotakis K, Vlachogianni T. Airborne particulate matter and human health: toxicological assessment and importance of size and composition of particles for oxidative damage and carcinogenic mechanisms. J Environ Sci Health C Environ Carcinog Ecotoxicol Rev 2008;26(4):339-62.
6) McGuinn LA, Schneider A, McGarrah RW, Ward-Caviness C, Neas LM, Di Q, et al. Association of long-term PM2.5 exposure with traditional and novel lipid measures related to cardiovascular disease risk. Environ Int 2019;122:193-200.
7) Brook RD, Rajagopalan S, Pope CA 3rd, Brook JR, Bhatnagar A, Diez-Roux AV, et al. Particulate matter air pollution and cardiovascular disease: an update to the scientific statement from the American Heart Association. Circulation 2010;121(21):2331-78.
8) Lin H, Qian ZM, Guo Y, Zheng Y, Ai S, Hang J, et al. The attributable risk of chronic obstructive pulmonary disease due to ambient fine particulate pollution among older adults. Environ Int 2018;113:143-8.
9) Wang BR, Shi JQ, Ge NN, Ou Z, Tian YY, Jiang T, et al. PM2.5 exposure aggravates oligomeric amyloid beta-induced neuronal injury and promotes NLRP3 inflammasome activation in an in vitro model of Alzheimer's disease. J Neuroinflammation 2018;15(1):132.
10) Chen S, Zhang Y, Wang Y, Lawrence WR, Rhee J, Guo T, et al. Long-term particulate matter exposure and the risk of neurological hospitalization: evidence from causal inference of a large longitudinal cohort in South China. Chemosphere 2023;345:140397.

11) Wang L, Luo D, Liu X, Zhu J, Wang F, Li B, et al. Effects of PM2.5 exposure on reproductive system and its mechanisms. Chemosphere 2021;264(Pt 1):128436.

12) Risom L, Møller P, Loft S. Oxidative stress-induced DNA damage by particulate air pollution. Mutat Res 2005;592(1-2):119-37.

13) Deng X, Zhang F, Rui W, Long F, Wang L, Feng Z, et al. PM2.5-induced oxidative stress triggers autophagy in human lung epithelial A549 cells. Toxicol In Vitro 2013;27(6):1762-70.

14) Lee DC, Choi H, Oh JM, Lee DH, Kim SW, Kim SW, et al. Protective effects of α-lipoic acid on cultured human nasal fibroblasts exposed to urban particulate matter. Int Forum Allergy Rhinol 2019;9(6):638-47.

15) Jin X, Xue B, Zhou Q, Su R, Li Z. Mitochondrial damage mediated by ROS incurs bronchial epithelial cell apoptosis upon ambient PM2.5 exposure. J Toxicol Sci 2018;43(2):101-11.

16) Wang Y, Zhong Y, Liao J, Wang G. PM2.5-related cell death patterns. Int J Med Sci 2021;18(4):1024-9.

17) Tang D, Kang R, Berghe TV, Vandenabeele P, Kroemer G. The molecular machinery of regulated cell death. Cell Res 2019;29(5):347-64.

18) Chen Y, Ye X, Escames G, Lei W, Zhang X, Li M, et al. The NLRP3 inflammasome: contributions to inflammation-related diseases. Cell Mol Biol Lett 2023;28(1):51.

19) Jia R, Wei M, Lei J, Meng X, Du R, Yang M, et al. PM2.5 induce myocardial injury in hyperlipidemic mice through ROS-pyroptosis signaling pathway. Ecotoxicol Environ Saf 2023;254:114699.

20) Chen W, Luo Y, Quan J, Zhou J, Yi B, Huang Z. PM2.5 induces renal tubular injury by activating NLRP3-mediated pyroptosis. Ecotoxicol Environ Saf 2023;265:115490.

21) Niu L, Li L, Xing C, Luo B, Hu C, Song M, et al. Airborne particulate matter (PM2.5) triggers cornea inflammation and pyroptosis via NLRP3 activation. Ecotoxicol Environ Saf 2021;207:111306.

22) Li J, An Z, Song J, Du J, Zhang L, Jiang J, et al. Fine particulate matter-induced lung inflammation is mediated by pyroptosis in mice. Ecotoxicol Environ Saf 2021;219:112351.

23) Wang Y, Tang N, Mao M, Zhou Y, Wu Y, Li J, et al. Fine particulate matter (PM2.5) promotes IgE-mediated mast cell activation through ROS/Gadd45b/JNK axis. J Dermatol Sci 2021;102(1):47-57.

24) Roseborough AD, Zhu Y, Zhao L, Laviolette SR, Pasternak SH, Whitehead SN. Fibrinogen primes the microglial NLRP3 inflammasome and propagates pro-inflammatory signaling via extracellular vesicles: implications for blood-brain barrier dysfunction. Neurobiol Dis 2023; 177:106001.

25) Ren F, Xu J, Zhang J, Xu X, Huang L, Sun W, et al. PM2.5 induced lung injury through upregulating ROS-dependent NLRP3 inflammasome-mediated pyroptosis. Immunobiology 2022;227(3):152207.

26) Zheng R, Tao L, Jian H, Chang Y, Cheng Y, Feng Y, et al. NLRP3 inflammasome activation and lung fibrosis caused by airborne fine particulate matter. Ecotoxicol Environ Saf 2018;163:612-9.

27) Li J, Zhang Y, Zhang L, An Z, Song J, Wang C, et al. Fine particulate matter exposure exacerbated nasal mucosal damage in allergic rhinitis mice via NLRP3 mediated pyroptosis. Ecotoxicol Environ Saf 2021;228:112998.

28) Li Y, Chang LH, Huang WQ, Bao HW, Li X, Chen XH, et al. IL-17A mediates pyroptosis via the ERK pathway and contributes to steroid resistance in CRSwNP. J Allergy Clin Immunol 2022;150(2):337-51.

29) Schantz MM, Cleveland D, Heckert NA, Kucklick JR, Leigh SD, Long SE, et al. Development of two fine particulate matter standard reference materials (<4 μm and <10 μm) for the determination of organic and inorganic constituents. Anal Bioanal Chem 2016;408(16):4257-66.